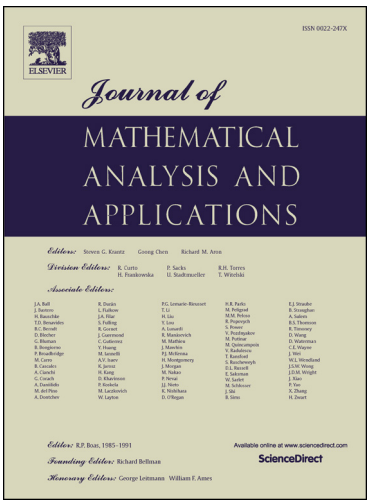
Accepted Manuscript



A cholera epidemic model in a spatiotemporally heterogeneous environment

Xueying Wang, Xiao-qiang Zhao, Jin Wang

PII: S0022-247X(18)30703-0
DOI: https://doi.org/10.1016/j.jmaa.2018.08.039
Reference: YJMAA 22496

To appear in: *Journal of Mathematical Analysis and Applications*

Received date: 24 August 2017

Please cite this article in press as: X. Wang et al., A cholera epidemic model in a spatiotemporally heterogeneous environment, *J. Math. Anal. Appl.* (2018), https://doi.org/10.1016/j.jmaa.2018.08.039

This is a PDF file of an unedited manuscript that has been accepted for publication. As a service to our customers we are providing this early version of the manuscript. The manuscript will undergo copyediting, typesetting, and review of the resulting proof before it is published in its final form. Please note that during the production process errors may be discovered which could affect the content, and all legal disclaimers that apply to the journal pertain.

ACCEPTED MANUSCRIPT

A cholera epidemic model in a spatiotemporally heterogeneous environment☆

Xueying Wang[a,*], Xiao-qiang Zhao[b], Jin Wang[c]

[a]*Department of Mathematics and Statistics, Washington State University, Pullman, WA 99163, USA*
[b]*Department of Mathematics and Statistics, Memorial University of Newfoundland, St. John's, NL A1C 5S7, Canada*
[c]*Department of Mathematics, University of Tennessee at Chattanooga, Chattanooga, TN 37403, USA*

Abstract

The transmission of cholera, a water- and food-borne intestinal infection, involves complex interactions among human hosts, pathogens, and the environment, and is impacted by the spatial variation and seasonal fluctuation. In this paper, we propose a new deterministic model to investigate the spatiotemporal dynamics of cholera transmission. The model employs a reaction-convection-diffusion system to represent the spatial movement of the hosts and pathogens, and incorporates time-periodic parameters to describe the seasonality of the disease transmission and bacterial growth rates. Using the theory of principle eigenvalues, we define and analyze the basic reproduction number of this model, based on which we establish the threshold type results for cholera transmission in a spatiotemporally heterogeneous environment.

Keywords: Cholera model, spatiotemporally, heterogeneous environments, threshold dynamics

1. Introduction

Cholera is a severe water- and food-borne infectious disease. The causing agent for human cholera is the bacterium *Vibrio cholerae*, which can be transmitted both from the contaminated aquatic environment (i.e., through indirect environment-to-human transmission route), and from person-to-person contacts such as shaking hands or eating food prepared by infected individuals (i.e., through direct human-to-human transmission route) [14, 21]. Thus, the dynamics of cholera involve multiple interactions among the human hosts, the pathogens, and the environment [22]. Although tremendous efforts have been made in the prevention, intervention and control of the disease, cholera remains a significant public health threat in underdeveloped countries and regions. The persistence of the disease has been highlighted by recent outbreaks in South Sudan (2014), Haiti (2010-2012), Zimbabwe (2008-2009), Angola (2006), South

*Corresponding author
Email address: xueying@math.wsu.edu (Xueying Wang)

ACCEPTED MANUSCRIPT

Africa (2000-2001), and many other places, which leads to more than 1.4 million cases of infection and about 28,000 deaths worldwide every year [43].

A large number of mathematical models have been published recently to improve our understanding of cholera dynamics (see, e.g., [1, 5, 6, 7, 8, 12, 13, 14, 21, 22, 23, 26, 30, 31, 35, 36]). Most of these models are based on relatively simple, autonomous ordinary differential equation (ODE) systems, where model parameters are constant in time and space, so that detailed mathematical analysis on stabilities and bifurcations can be conducted. In particular, the basic reproduction number R_0 has been established as a sharp threshold for disease dynamics in a large class of these cholera models. Practically, however, spatial and temporal heterogeneities, which involve distinctions in ecological and geographical environments, population characteristics, and socioeconomic structures, cause variations in the disease contact rates, human activity levels, pathogen growth and death rates, etc., which in turn have strong impact on cholera dynamics. Consequently, several important questions regarding the epidemiology of cholera remain to be answered. For example, what factors shape the distribution of cholera that persists in some countries/regions but not in others? Why does cholera typically proliferate in a certain period of the year (such as the rainy or monsoon seasons [17, 38])? How does the movement of hosts and pathogens impact the transmission and spread of cholera? And how to quantify the infection risk of cholera in an environment with spatiotemporal heterogeneities?

Several studies have already been devoted to the spatial dynamics of cholera transmission. ODE models based on patch/network structures were studied in [12, 27, 32]. Models based on partial differential equations (PDEs) were also introduced to investigate cholera epidemics with the movement of human hosts and the dispersal of pathogens [4, 7, 25, 34, 36, 40, 41], among which threshold dynamics of cholera epidemics were established using a reaction-convection-diffusion model in homogeneous environments [40, 41]. Meanwhile, a few efforts have been made to investigate the seasonal dynamics of cholera. In [8], simple numerical tests were conducted for three scenarios with time-periodic parameters, in addition to the main discussion on the autonomous cholera model. The authors of [23] proposed and analyzed a general ODE system that incorporates seasonality into cholera epidemics. These studies, focused on either the spatial heterogeneities or the seasonal fluctuations (but not both), have certainly produced many useful results and have improved our understanding of cholera dynamics. Practically, however, the spatial and temporal components are always coupled with each other in shaping the pattern of cholera transmission and spread, and such complex, coupled disease dynamics may not be best represented by separated spatial or temporal modeling approaches.

In this paper, we aim to investigate the spatiotemporal dynamics of cholera using a single modeling framework. Our goal is to develop a holistic cholera modeling approach that can represent the interaction among climatic, geographical, ecological, and biological factors in the evolution of cholera epidemics. To that end, our current research task is built on the models developed, and knowledge gained, from the separated, spatial or temporal, modeling approaches. We will construct a reaction-convection-diffusion PDE

ACCEPTED MANUSCRIPT

system with time-periodic contact/growth rates to incorporate both the seasonal and spatial impacts, with an aim to provide new and deeper insight into cholera dynamics that cannot be gained otherwise through separated spatial and temporal analysis.

Throughout this paper, we will focus our attention on characterizing the threshold dynamics of cholera in a spatiotemporally heterogeneous environment. We will utilize the basic reproduction number, commonly denoted by R_0 , as the main analytical tool. The definition and analysis of the basic reproduction number for autonomous ODE-based epidemic models, using the next-generation matrices, have been well established [10, 33]. Several extensions of this framework have been made, for example, to time-periodic ODE systems [2, 37], to reaction-diffusion PDE systems [39], to epidemic models with time delay [16, 42], and to reaction-diffusion SIS (susceptible-infected-susceptible) models with time-periodic coefficients [20]. In the current study, we will further extend the concept of the basic reproduction number to periodic, reaction-convection-diffusion PDE systems, incorporating the SIRS (susceptible-infected-recovered-susceptible) host compartments and a significant environmental component that describes the dynamics of the water-borne pathogen. We will conduct a rigorous analysis for the R_0 of our cholera model, using the principal eigenvalue theory [3, 18, 29], and perform a careful numerical study for a range of model parameters.

We organize the remainder of this paper as follows. In Section 2 we describe the details of our periodic PDE model for cholera. In Section 3 we introduce the basic reproduction number for our model and characterize its main properties. Using the basic reproduction number, we study the threshold dynamics of our cholera model in Section 4. In addition, we present numerical simulation results for the variation of R_0 under different spatial and temporal scenarios. Finally, we conclude the paper with a brief discussion.

2. The Model

Consider a cholera PDE model along a theoretical river

$$\begin{aligned}
\frac{\partial S}{\partial t} &= \Lambda - S\beta_1(x,t)I - S\beta_2(x,t)\frac{B}{B+K} - d\,S + \sigma R + D_1\frac{\partial^2 S}{\partial x^2}, && 0<x<1,\ t>0,\\
\frac{\partial I}{\partial t} &= S\beta_1(x,t)I + S\beta_2(x,t)\frac{B}{B+K} - (d+\gamma)I + D_2\frac{\partial^2 I}{\partial x^2}, && 0<x<1,\ t>0,\\
\frac{\partial R}{\partial t} &= \gamma I - (d+\sigma)R + D_3\frac{\partial^2 R}{\partial x^2}, && 0<x<1,\ t>0,\\
\frac{\partial B}{\partial t} &= \xi(x,t)I + g(x,t)B\left(1-\frac{B}{K_B}\right) - \delta B - v\frac{\partial B}{\partial x} + D_4\frac{\partial^2 B}{\partial x^2}, && 0<x<1,\ t>0,
\end{aligned} \tag{1}$$

with no flux boundary condition

$$\begin{aligned}
&\frac{\partial U}{\partial x}(0,t) = \frac{\partial U}{\partial x}(1,t) = 0, \quad U = S, I, R\,, \quad t>0,\\
&D_4\frac{\partial B}{\partial x}(x,t) - vB(x,t) = 0, \quad x = 0,\ 1, \quad t>0,
\end{aligned} \tag{2}$$

ACCEPTED MANUSCRIPT

and the initial condition

$$U(x,0) = U_0(x) \geq 0, \quad U = S, I, R, B, \quad 0 \leq x \leq 1. \tag{3}$$

Here $x \in [0,1]$ is the position variable and $t \geq 0$ is the time variable. $x = 0$ and 1 represent two ends of the river. $S = S(x,t), I = I(x,t)$, and $R = R(x,t)$ measure the densities of susceptible, infectious, and recovered human hosts at location x and time t, respectively. $B = B(x,t)$ denotes the concentration of cholera in the water environment. Λ is the influx rate of susceptible humans. D_i $(1 \leq i \leq 4)$ is the diffusion coefficient of S, I, R and B, respectively. v is the convection coefficient depicting the drift for vibrio's transport. d is the natural death rate of human hosts. β_1 and β_2 represent the direct (due to human-to-human contact) and indirect transmission (due to environment-to-human contact) rates, respectively, K is the half saturation constant that describes the infectious dose in water sufficient to produce disease in 50% of those exposed. $g(x,t)$ is intrinsic growth rate of the bacteria. K_B denotes the maximal capacity of the free-living bacteria in the environment, σ is the rate at which recovered individuals lose immunity, γ represents the recovery rate of infectious hosts, and ξ denotes the time-dependent shedding rate of bacteria by infectious human hosts, and δ is the natural death rate of the bacteria.

Let $Z = C([0,1], \mathbb{R})$ and $Z^+ = C([0,1], \mathbb{R}_+)$. Let $U_0(x) = U(x,0)$ for all $x \in [0,1]$, where $U = S, I, R, B$. We assume that

(H1) S_0, I_0, R_0 and $B_0 \in Z^+$,
(H2) $I_0 \not\equiv 0$ or $B_0 \not\equiv 0$ on $[0,1]$;
(H3) $\beta_1(x,t)$ $\beta_2(x,t)$, $\xi(x,t)$ and $g(x,t)$ are positive Hölder continuous functions defined on $[0,1] \times \mathbb{R}$, and ω-periodic in time.

By the classical theory on parabolic equations, system (1) admits a unique classical solution

$$(S, I, R, B) \in C^{2,1}([0,1] \times (0, \infty)).$$

Moreover, one can derive that $S(x,t)$, $I(x,t)$, $R(x,t)$ and $B(x,t)$ are all positive on $[0,1] \times (0,\infty)$ by applying the strong maximal principle and Hopf boundary lemma for parabolic systems (see, e.g., [24, Theorems 4 and 3]).

2.1. A conserved population

Write

$$N(t) = \int_0^1 (S + I + R)(x,t)dx, \tag{4}$$

which measures the total number of human hosts over the entire domain $[0,1]$ at time t. It is apparent that $N_0 := N(0) > 0$.

We first consider a special case where the influx of susceptibles is solely based on newborns and where the natural birth and death rates are equal (both denoted by d).

ACCEPTED MANUSCRIPT

Effectively, we replace the influx rate Λ in system (1) by dN, and obtain

$$\frac{d}{dt}N(t) = \int_0^1 \left(D_1 \frac{\partial^2 S}{\partial x^2} + D_2 \frac{\partial^2 I}{\partial x^2} + D_3 \frac{\partial^2 R}{\partial x^2} \right) dx = \left[D_1 \frac{\partial S}{\partial x} + D_2 \frac{\partial I}{\partial x} + D_3 \frac{\partial R}{\partial x} \right] \Big|_{x=0}^{x=1} = 0. \tag{5}$$

It implies that the total human population size stays at a constant; that is,

$$N(t) \equiv N_0, \quad \forall t \geq 0, \tag{6}$$

and this also shows that $\|S(\cdot,t)\|_{L^1([0,1])}, \|I(\cdot,t)\|_{L^1([0,1])}, \|R(\cdot,t)\|_{L^1([0,1])}$ are uniformly bounded for $t \geq 0$. Particularly,

$$\|I\|_{L^1([0,1])} \leq \theta_0 \tag{7}$$

for some positive constant θ_0. Hence

$$\begin{aligned} \frac{d}{dt}\int_0^1 B(x,t)dx &= \int_0^1 \xi(x,t)I + g(x,t)B\left(1 - \frac{B}{K_B}\right) - \delta B - v\frac{\partial B}{\partial x} + D_4 \frac{\partial^2 B}{\partial x^2} \\ &\leq \xi^* \theta_0 + \theta_1 - r\int_0^1 B(x,t)dx \end{aligned} \tag{8}$$

where $\xi^* = \max\{\xi(x,t) : 0 \leq x \leq 1, 0 \leq t \leq \omega\}$. We have used the facts (a) there exists positive constants θ_1 and r such that

$$g(x,t)B\left(1 - \frac{B}{K_B}\right) - \delta B \leq \theta_1 - rB, \quad \forall B \geq 0, \tag{9}$$

and (b)

$$\int_0^1 \left(-v\frac{\partial B}{\partial x} + D_4 \frac{\partial^2 B}{\partial x^2} \right) dx = \left(-vB + D_4 \frac{\partial B}{\partial x} \right) \Big|_{x=0}^{x=1} = 0. \tag{10}$$

Equation (8) yields

$$\frac{d}{dt}\int_0^1 B(x,t)dx \leq \theta - r\int_0^1 B(x,t)dx \tag{11}$$

with $\theta = \xi^*\theta_0 + \theta_1$. This gives

$$\begin{aligned} \textstyle\int_0^1 B(x,t)dx &\leq \textstyle\int_0^1 B(x,0)dx\ e^{-rt} + \frac{\theta}{r}(1 - e^{-rt}) \\ &\leq \max\left\{ \textstyle\int_0^1 B(x,0)dx,\ \theta/r \right\}, \qquad t \geq 0. \end{aligned} \tag{12}$$

Then (12) yields

$$\limsup_{t\to\infty} \int_0^1 B(x,t)dx \leq \frac{\theta}{r}, \tag{13}$$

which is independent of initial data. Namely, $\|B(\cdot,t)\|_{L^1([0,1])} \leq C_B$ for all $t \geq 0$ and $\|B(\cdot,t)\|_{L^1([0,1])} \leq C_{B_T}$ for $t \geq T$, where C_B depends on the initial data and C_{B_T} is independent of initial data when T is large enough.

ACCEPTED MANUSCRIPT

Lemma 2.1. *The system* (1) *has a unique* ω*-periodic DFE solution, i.e.,* $(N_0, 0, 0, 0)$.

Proof. Clearly, $X_0 = (N_0, 0, 0, 0)$ is a DFE. It remains to verify that it is unique. Let $(\bar{S}(x), 0, \bar{R}(x), 0)$ denote an arbitrary DFE of (1). The equations (1) imply that

$$\begin{aligned} &\frac{\partial^2}{\partial x^2}(D_1\bar{S} + D_3\bar{R}) = 0, \ \forall x \in (0,1), \\ &\frac{\partial}{\partial x}(D_1\bar{S} + D_3\bar{R}) = 0, \ x = 0, 1. \end{aligned} \tag{14}$$

Thus, $D_1\bar{S} + D_3\bar{R}$ is a constant. By the third equation of (1) , $\bar{R} = 0$ when $\bar{I} = 0$. Then equation (6) implies that $\bar{S} = N_0$. □

2.2. A varying total population

In general, the total population size would vary over time. By (1), we have

$$\frac{dN}{dt} = \Lambda - d\,N(t). \tag{15}$$

In view of $N(t) = N_0 e^{-dt} + \Lambda\,(1 - e^{-dt})/d \le \max\{N_0,\ \Lambda/d\}$ for all $t \ge 0$ and $\lim\limits_{t\to\infty} N(t) = \Lambda/d$, we see that

$$\begin{aligned} &\|S\|_{L^1([0,1])} + \|I\|_{L^1([0,1])} + \|R\|_{L^1([0,1])} + \|B\|_{L^1([0,1])} \le \tilde{C}_1, \quad t \ge 0, \\ &\|S\|_{L^1([0,1])} + \|I\|_{L^1([0,1])} + \|R\|_{L^1([0,1])} + \|B\|_{L^1([0,1])} \le \tilde{C}_2, \quad t \ge T, \end{aligned} \tag{16}$$

where $\tilde{C}_1 > 0$ is a constant depending on initial data and $\tilde{C}_2 > 0$ is a constant independent of initial data when T is sufficiently large.

3. Basic Reproduction Number

An important disease threshold in epidemiology is the basic reproduction number R_0, which measures the average number of secondary infection when one primary infectious case is introduced into the host virgin population. The theory of R_0 has been well established for autonomous and periodic ODE models with compartmental structure [33, 37]. This concept has also been extended to periodic reaction-diffusion epidemic models (see, e.g., [37, 20]).

To introduce the basic reproduction number for our model system, we need some notations. Let $X = C([0,1], \mathbb{R}^4)$ denote the Banach space equipped with supremum norm. Let $X^+ = C([0,,1], \mathbb{R}^4_+)$. (X, X^+) are strongly ordered. Let C_ω denote the ordered Banach space of all continuous functions from $\mathbb{R}$ to X of period ω, equipped with the supernorm $\|\cdot\|$ and the positive cone $C^+_\omega = \{g \in C_\omega : g(t)(x) \ge 0,\ t \in \mathbb{R},\ \forall x \in [0,1]\}$. In our cholera model, the disease components are I and B. If we linearize this

ACCEPTED MANUSCRIPT

system at the DFE, the associated reaction-advection-diffusion equation with I and B is given by

$$\begin{aligned}
&\frac{\partial I}{\partial t} = D_2\frac{\partial^2 I}{\partial x^2} + N\beta_1(x,t)I + N\beta_2(x,t)/KB - (d+\gamma)I,\\
&\frac{\partial B}{\partial t} = D_4\frac{\partial^2 B}{\partial x^2} - v\frac{\partial B}{\partial x} + \xi(x,t)I + g(x,t)B - \delta B,\\
&\frac{\partial I}{\partial x}(0,t) = \frac{\partial I}{\partial x}(1,t) = 0,\\
&\left(D_4\frac{\partial B}{\partial x} - vB\right)(0,t) = \left(D_4\frac{\partial B}{\partial x} - vB\right)(1,t) = 0,
\end{aligned} \tag{17}$$

for $x \in [0,1]$ and $t > 0$.

Let $Y(t,s)$ be the evolution operator of the following linear reaction-advection-diffusion equation:

$$\begin{aligned}
&\frac{\partial I}{\partial t} = D_2\frac{\partial^2 I}{\partial x^2} - (d+\gamma)I,\\
&\frac{\partial B}{\partial t} = D_4\frac{\partial^2 B}{\partial x^2} - v\frac{\partial B}{\partial x} - \delta B,\\
&\frac{\partial I}{\partial x}(0,t) = \frac{\partial I}{\partial x}(1,t) = 0,\\
&\left(D_4\frac{\partial B}{\partial x} - vB\right)(0,t) = \left(D_4\frac{\partial B}{\partial x} - vB\right)(1,t) = 0,
\end{aligned} \tag{18}$$

for $x \in [0,1]$ and $t > 0$.

Write

$$F(x,t) = \begin{pmatrix} N\beta_1(x,t) & N\beta_2(x,t)/K \\ \xi(x,t) & g(x,t) \end{pmatrix} \quad \text{and} \quad V = \begin{pmatrix} d+\gamma & 0 \\ 0 & \delta \end{pmatrix} \tag{19}$$

for which F captures the new infection and V represents the transmission.

By (H3), $\beta_2(x,t) > 0$ and $\xi(x,t) > 0$ for $x \in [0,1]$ and $t > 0$. Hence, F is cooperative and irrreducible and $-V$ is cooperative.

By the standard semigroup theory, there exists $M > 0$ and $r > 0$ s.t.

$$\|Y(t,s)\| \le Me^{-r(t-s)}, \quad \forall t \ge s. \tag{20}$$

Suppose $\phi(x,s) = (I(x,t), B(x,t))^T$ is the joint density distribution of the infectious human hosts and bacteria in the spatial position $x \in [0,1]$ at time s. Then $F(x,s)\phi(x,s)$ gives the density distribution of new infections produced by the primary infectious individuals that were introduced at time s. Thus, the next generation operator $L : C_\omega \to C_\omega$ is given by

$$\big(L\phi\big)(t) = \int_{-\infty}^{t} Y(t,s)F(\cdot,s)\phi(\cdot,s)ds = \int_0^{\infty} Y(t,t-\tau)F(\cdot,t-\tau)\phi(\cdot,t-\tau)d\tau. \tag{21}$$

ACCEPTED MANUSCRIPT

This operator denotes the the cumulative density distribution of new infections at position x and time t. Under our hypotheses, one can verify that L is continuous and compact on C_ω. Moreover, it is positive; that is, $L(C_\omega^+) \subset C_\omega^+$.

It is worth to mention that there is another linear operator defined by

$$\big(\hat{L}\phi\big)(t) = \int_0^\infty F(\cdot,t)Y(t,t-\tau)\phi(\cdot,t-\tau)d\tau = F(\cdot,t)\int_0^\infty Y(t,t-\tau)\phi(\cdot,t-\tau)d\tau. \quad (22)$$

For any $\tau > 0$, $Y(t,t-\tau)\phi(\cdot,t-\tau)$ represents the distribution of infectious cases introduced at $t-\tau$ and remaining to be infected at time t. Hence $\int_0^\infty Y(t,t-\tau)\phi(\cdot,t-\tau)d\tau$ is the distribution of accumulated infectious cases up to time t and remaining to be infected at time t. Thus,

$$F(\cdot,t)\int_0^\infty Y(t,t-\tau)\phi(\cdot,t-\tau)d\tau$$

gives the distribution of newly infected cases at time t. The spectral radius of this operator, $\rho\big(\hat{L}\big)$, is also referred to as the basic reproduction number. Let's write

$$\big(\mathcal{A}\phi\big)(t) = \int_0^\infty Y(t,t-\tau)\phi(\cdot,t-\tau)d\tau, \quad (23)$$

and

$$\big(\mathcal{B}\phi\big)(t) = F(\cdot,t)\phi(\cdot,t). \quad (24)$$

Clearly, $L = \mathcal{A}\circ\mathcal{B}$ and $\hat{L} = \mathcal{B}\circ\mathcal{A}$. It follows immediately from $\rho(\mathcal{A}\circ\mathcal{B}) = \rho(\mathcal{B}\circ\mathcal{A})$ that $\rho(L) = \rho\big(\hat{L}\big)$. In other words, these two linear operators give the same basic reproduction number although they have different biological interpretations.

Motivated by the concept of next generation operators in [2, 20, 29, 37], the basic reproduction number R_0 is defined to be the spectral radius as follows:

$$R_0 = \rho(L) = \rho\big(\hat{L}\big). \quad (25)$$

To study local stability of the DFE, we will need to consider the following eigenvalue problem

$$\begin{array}{ll} \dfrac{\partial W}{\partial t} - \mathcal{G}W - F(x,t)W = \mu W, & x\in(0,1), t>0,\\ \mathcal{B}W = 0, & x = 0,1,\ t>0,\\ W(x,0) = W(x,\omega) = (I_0(x), B_0(x))^T, & 0<x<1. \end{array} \quad (26)$$

where the definition of F is given in (19) and

$$\mathcal{G} = \begin{pmatrix} D_2\dfrac{\partial^2}{\partial x^2} - (d+\gamma) & 0\\ 0 & D_4\dfrac{\partial^2}{\partial x^2} - v\dfrac{\partial}{\partial x} - \delta \end{pmatrix}, \quad \mathcal{B} = \begin{pmatrix} \dfrac{\partial}{\partial x}\\ D_4\dfrac{\partial}{\partial x} - v \end{pmatrix}. \quad (27)$$

ACCEPTED MANUSCRIPT

Let $U(t,s)$ denote the evolution operators of

$$\begin{aligned} &\frac{\partial \Phi}{\partial t} = \mathcal{G}\Phi + F(x,t)\Phi, \quad x \in (0,1), t > 0. \\ &\mathcal{B}\Phi = 0, \qquad\qquad\qquad\quad x = 0, 1,\ t > 0. \end{aligned} \tag{28}$$

Since $U(\omega, 0)$ is compact and strongly positive, the eigenvalue problem associated with the linear system (28) has a principle eigenvalue μ_0 (see, e.g., [18]). By the general result [29], we have the following observation.

Lemma 3.1. *$1 - R_0$ has the same sign as μ_0.*

Proof. Let $\mathcal{W}(U)$ be the exponential growth bound of the evolution family $U(t,s)$, i.e.,

$$\mathcal{W}(U) = \inf\left\{r : \exists M > 1,\ s.t.\ \|U(t+s,s)\| \le Me^{rt}\right\}. \tag{29}$$

By the same argument as in [18], it easily follows that

$$\mu_0 = -\frac{\log \rho(U(\omega, 0))}{\omega}. \tag{30}$$

Meanwhile, applying [29, Proposition 5.5] yields

$$\mathcal{W}(U) = \frac{\log \rho(U(\omega, 0))}{\omega}. \tag{31}$$

Thus, (30) and (31) imply that $\mu_0 = -\mathcal{W}(U)$. On the other hand, we note that $\mathcal{W}(Y) < 0$, where Y is the evolution family of (18). It then follows from [29, Theorem 5.7] that $\rho\big(\hat{L}\big) - 1$ has the same sign as $\mathcal{W}(U)$. In view of $R_0 = \rho(L) = \rho\big(\hat{L}\big)$, $1 - R_0$ and μ_0 have the same sign. □

Note that the definition of R_0 (25) rarely has an analytical expression, and it is usually difficult to numerically compute R_0 using this definition. The following result offers another characterization of R_0, which provides an approach to numerically evaluating R_0.

Lemma 3.2. *If $R_0 > 0$, then $\dfrac{1}{R_0}$ is the principle eigenvalue of the following linear periodic-parabolic eigenvalue problem:*

$$\begin{aligned} &\frac{\partial W}{\partial t} = \mathcal{G}W + \lambda F(x,t)W, && x \in (0,1), t > 0, \\ &\mathcal{B}W = 0, && x = 0, 1,\ t > 0, \\ &W(x,0) = W(x,\omega) = (I_0(x), B_0(x))^T, && 0 < x < 1. \end{aligned} \tag{32}$$

for all $x \in [0,1]$ and $t \in [0,\omega]$ with parameter $\lambda > 0$.

ACCEPTED MANUSCRIPT

Proof. For any given $\lambda > 0$, let $\mu_0(\lambda)$ denote the principle eigenvalue of the following linear periodic eigenvalue problem

$$\begin{aligned} &\frac{\partial \Psi}{\partial t} = \mathcal{G}\Psi + \lambda F(x,t)\Psi + \mu\Psi, && x \in (0,1), t > 0, \\ &\mathcal{B}\Psi = 0, && x = 0, 1,\ t > 0, \\ &\Psi(x,0) = \Psi(x,\omega) = (I_0(x), B_0(x))^T, && 0 < x < 1. \end{aligned} \tag{33}$$

Since $R_0 > 0$, the basic reproduction number of the model with $F(x,t)$ replaced by $\frac{1}{R_0}F(x,t)$ is $\frac{1}{R_0}R_0 = 1$. By Lemma 3.1, we then have $\mu_0(1/R_0) = 0$. As argued in [3, Lemmas 3.1 and 3.2], it follows that $\mu_0(\lambda)$ is a concave function. Since $\mu_0(0+) > 0$ and $\mu_0(1/R_0) = 0$, $1/R_0$ is the unique positive root of $\mu_0(\lambda)$, and hence $1/R_0$ is the principle eigenvalue of the problem (32). □

Remark: If Dirichlet or Robin-type boundary condition is used in system (1)*, Lemma 3.2 is still valid with the associated $\mathcal{B}$. It is worth mentioning that R_0 will be affected by the boundary condition.*

4. Threshold Dynamics

In this section, we establish the global dynamics of (1) in terms of R_0.

Theorem 4.1. *Suppose that either (C1) $D_1 = D_2 = D_3 = D$ or (C2) $\sigma = 0$. If $R_0 < 1$, then system* (1) *admits a unique global nonnegative solution $u(x,t;\phi) = (S,I,R,B)(x,t)$ with $\phi = (S_0, I_0, R_0, B_0) \in X^+$. Moreover,*

$$\lim_{t\to\infty} u(x,t;\phi) = (\bar{N}, 0, 0, 0), \tag{34}$$

for all $\phi \in X^+$, where $\bar{N} = \Lambda/d$.

Proof. First, let's consider the following eigenvalue problem

$$\begin{aligned} &\frac{\partial V}{\partial t} - \mathcal{G}V - \hat{F}^\epsilon(x,t)V = \mu V, && x \in (0,1), t > 0. \\ &\mathcal{B}V = 0, && x = 0, 1,\ t > 0 \\ &V(x,0) = V(x,\omega) = (I_0(x), B_0(x))^T, && 0 < x < 1. \end{aligned} \tag{35}$$

with G and B defined in (27), and

$$\hat{F}^\epsilon(x,t) = \begin{bmatrix} \beta_1(x,t)(N+\epsilon) & \beta_2(x,t)(N+\epsilon)/K \\ \xi(x,t) & g(x,t) \end{bmatrix}. \tag{36}$$

and $V = (V_I, V_B)^T$. This problem (35) has a unique principle eigenvalue $\mu_\epsilon = \mu(N+\epsilon) > 0$ with a positive eigenfunction $V_\epsilon(x,t)$ for $\epsilon > 0$ sufficiently small. Since $R_0 < 1$, it follows from Lemma 3.1 that $\mu_0 > 0$. By $\lim_{\epsilon\to 0}\mu_\epsilon = \mu_0$, one can choose a $\epsilon_0 > 0$ sufficiently small such that $\mu_{\epsilon_0} > 0$.

ACCEPTED MANUSCRIPT

Suppose that (C1) $D_1 = D_2 = D_3 = D$ holds. Adding the first three equations of (1) leads to

$$\begin{aligned} &\frac{\partial n}{\partial t} = \Lambda - d\, n + D\frac{\partial^2 n}{\partial x^2}, && 0 < x < 1,\, t > 0. \\ &\frac{\partial n}{\partial x}(0,t) = \frac{\partial n}{\partial x}(1,t), && t > 0, \\ &n(x,0) = (S_0 + I_0 + R_0)(x), && 0 \le x \le 1. \end{aligned} \tag{37}$$

It is known that system (37) has a unique positive equilibrium $\bar{N} = \Lambda/d$ that is globally asymptotically stable in $C([0,1],\mathbb{R})$, i.e.,

$$\lim_{t\to\infty} n(x,t) = \bar{N}. \tag{38}$$

Since $S, I, R \ge 0$, for the fixed $\epsilon_0 > 0$, there exists $t_0 = t_0(\epsilon_0) > 0$, such that for all $t \ge t_0$, $x \in [0,1]$,

$$S(x,t) \le \bar{N} + \epsilon_0. \tag{39}$$

Or assume that (C2) $\sigma = 0$ is satisfied. Then the first equation of (1) yields

$$\frac{\partial S}{\partial t} \le \Lambda - d\, S + D_1\frac{\partial^2 S}{\partial x^2}. \tag{40}$$

By the comparison principle, it is easy to see that (39) is true. Hence in either case,

$$\frac{\partial I}{\partial t} \le \beta_1(x,t)(\bar{N}+\epsilon_0)I + \beta_2(x,t)(\bar{N}+\epsilon_0)\frac{B}{K} - (d+\gamma)I + D_2\frac{\partial^2 I}{\partial x^2} \tag{41}$$

and

$$\frac{\partial B}{\partial t} \le \xi(x,t)I + g(x,t)B - \delta B - v\frac{\partial B}{\partial x} + D_4\frac{\partial^2 B}{\partial x^2} \tag{42}$$

using the second and third equations of (1). One can verify by simple analysis that, for $\eta > 0$ sufficiently large,

$$(I_0(x), B_0(x)) \le \eta V_{\epsilon_0}(x), \quad 0 \le x \le 1. \tag{43}$$

Hence $\eta e^{-\mu_{\epsilon_0} t} V_{\epsilon_0}(x,t)$ is a supersolution of the following problem

$$\begin{aligned} &\frac{\partial V}{\partial t} - \mathcal{G}V - \hat{F}^{\epsilon_0}V = 0, && x \in (0,1), t > 0. \\ &\mathcal{B}V = 0, && x = 0, 1,\, t > 0 \\ &V(x,0) = (I_0(x), B_0(x))^T, && 0 < x < 1. \end{aligned} \tag{44}$$

This yields

$$(I(x,t), B(x,t)) \le \eta e^{-\mu_{\epsilon_0} t} V_{\epsilon_0}(x,t), \quad 0 < x < 1,\ t > 0. \tag{45}$$

Applying the comparison principle, we see that

$$\lim_{t\to\infty}(I(x,t), B(x,t)) = (0,0), \quad 0 < x < 1. \tag{46}$$

ACCEPTED MANUSCRIPT

Now let's consider the equation for R. By (45), there exists $C_R > 0$ such that

$$\frac{\partial R}{\partial t} - D_3 \frac{\partial^2 R}{\partial x^2} + (d+\sigma)R = \gamma I \le C_R e^{-\mu_{\epsilon_0} t}. \tag{47}$$

Since the right hand side decays to zero exponentially fast,

$$\lim_{t\to\infty} R(x,t) = 0, \quad 0 < x < 1. \tag{48}$$

It remains to consider the asymptotic behavior of S as $t \to \infty$. From the equation of S, we have

$$\frac{\partial S}{\partial t} - D_1 \frac{\partial^2 S}{\partial x^2} - \Lambda + d\, S = -\sigma R + S(\beta_1 I + \beta_2 B/(B+K)). \tag{49}$$

In view of (46) and (48), the right side of (49) goes to zero as $t \to \infty$. Hence (49) is asymptotic to

$$\begin{aligned} &\frac{\partial \bar{S}}{\partial t} = D_1 \frac{\partial^2 \bar{S}}{\partial x^2} + \Lambda - d\,\bar{S}, \quad 0 < x < 1,\, t > 0, \\ &\frac{\partial \bar{S}}{\partial x} = 0, \qquad\qquad\qquad\quad t > 0, \\ &\bar{S}(x,0) = S_0(x), \qquad\qquad 0 \le x \le 1, \end{aligned} \tag{50}$$

as $t \to \infty$. It is known that this equation equipped with Neumann boundary condition admits a unique positive steady state $\bar{N} = \Lambda/d$ and it is globally asymptotically stable in $C([0,1],\mathbb{R})$. Therefore, by the theory of asymptotic autonomous semiflow [28, Corollary 4.3], we further have

$$\lim_{t\to\infty} S(x,t) = \bar{N}, \quad 0 < x < 1. \tag{51}$$

□

Remark: Condition (C1) implies that human hosts have homogeneous diffusion. (C2) assumes that the immunity loss of human hosts can be neglected. These conditions have certain restrictions. Nevertheless, for cholera, the majority of infections are minor and asymptomatic, and the asymptomatic individuals are typically above 90% among all infected individuals (see, e.g., [15]). Hence, it might be reasonable to assume that most infected individuals have the same level of mobility as that of the susceptible and recovered individuals, which (approximately) leads to condition (C1). Meanwhile, the immunity of cholera generally lasts about 5 years. If we consider a relatively short time frame, such as the duration of a typical cholera outbreak (ranging from several months to one year), then we might assume that the immunity loss can be neglected; i.e., condition (C2) holds.

In what follows, we shall focus on the dynamical behavior of the system (1) when $R_0 > 1$. Our first aim is to establish the uniform boundedness of the solutions of this system. As a direct application [11, Theorem 1, Corollary 1], we have the following result:

ACCEPTED MANUSCRIPT

Lemma 4.2. *Let's consider the following system of quasilinear parabolic equations*

$$\begin{aligned} &\frac{\partial u_i}{\partial t} = D_i \frac{\partial^2 u_i}{\partial x^2} - \nu_i \frac{\partial u_i}{\partial x} + f_i(t,x,u), && x \in (0,1),\ t>0, \\ &D_i \frac{\partial u_i}{\partial x} - \nu_i u_i = 0, && x = 0,1,\ t>0, \\ &u_i(x,0) = u_i^0(x), && x \in [0,1], \end{aligned} \tag{52}$$

where $u = (u_1, \cdots, u_m)$, $u^0 = (u_i^0, \cdots, u_m^0)$ *with each* $u_i^0 \in C([0,1])$ *and* $D_i > 0$ *and* $\nu_i \geq 0$ *for* $i = 1, 2, \cdots, m$. *For each* $1 \leq i \leq m$,

$$|f_i(t,x,u)| \leq C_1 \sum_{i=1}^{m} |u_i|^\sigma + C_2, \tag{53}$$

for some constants $C_1 \geq 0, C_2 \geq 0$ *and* $\sigma > 0$. *Let* p_0 *denote a positive constant such that*

$$p_0 > \frac{m}{2} \max\{0, \sigma - 1\}.$$

Let $\tau(u^0)$ *denote the maximal existence time of the solution* $u = u(t,x;u_0)$.

If there exists a positive function $C_{p_0}(u^0)$ *such that*

$$\|u(t,\cdot)\|_{L^{p_0}([0,1])} \leq C_{p_0}(u^0), \quad \forall\, 0 < t < \tau(u_0),$$

then the solution u *exists for all* $t > 0$ *and there exists a positive function* $C_\infty(u_0)$ *such that*

$$\|u(t,\cdot)\|_{L^\infty([0,1])} \leq C_\infty(u^0), \quad \forall\, t > 0.$$

Furthermore, if there are constant t_0 *and* K_{t_0} *independent of initial data such that*

$$\|u(t,\cdot)\|_{L^{p_0}([0,1])} \leq K_{p_0}(t_0), \quad \forall\, t \geq t_0,$$

then there exists a positive function $K_\infty(t_0)$ *such that*

$$\|u(t,\cdot)\|_{L^\infty([0,1])} \leq K_\infty(t_0), \quad \forall\, t \geq t_0.$$

The following result follows directly from Lemma 4.2 by taking $\sigma = 1$, $p_0 = 1$ and $t_0 = T$.

Lemma 4.3. *There exists positive constants* C_1, C_2 *and* $T > 0$ *such that, the solution* $u = (S, I, R, B)$ *of* (1) *satisfies*

$$\|S\|_{L^\infty([0,1])} + \|I\|_{L^\infty([0,1])} + \|R\|_{L^\infty([0,1])} + \|B\|_{L^\infty([0,1])} \leq C_1, \quad t \geq 0,$$

and

$$\|S\|_{L^\infty([0,1])} + \|I\|_{L^\infty([0,1])} + \|R\|_{L^\infty([0,1])} + \|B\|_{L^\infty([0,1])} \leq C_2, \quad t \geq T,$$

where C_1 *depends on the initial data, and* C_2 *is independent of initial data if* T *is sufficiently large.*

ACCEPTED MANUSCRIPT

Theorem 4.4. *If $R_0 > 1$, then system (1) admits at least one positive periodic solution and there exists $\eta > 0$ such that any solution of this system $u(x,t) := (u_1, u_2, u_3, u_4)(x,t)$ satisfies*

$$\liminf_{t\to\infty} u_i(x,t) \geq \eta, \quad \forall i = 1,2,3,4 \tag{54}$$

uniformly on $[0,1]$.

Proof. We will proceed to prove these assertions by using the persistent theory [44, 19]. By the classical regularity theory of parabolic equations, we know that, for every initial $u_0 := (S_0, I_0, R_0, B_0) \in X^+$, system (1) has a unique solution $u(\cdot,t,u^0) := (S,I,R,B)(\cdot,t)$ on $[0,\infty)$ with $u(\cdot,0,u_0) = u_0(\cdot)$. One can now define the associated ω-periodic semiflow $\Phi_t : X^+ \to X^+$, which is given by

$$\Phi_t\big(u_0(\cdot)\big) = u(\cdot,t,u_0), \quad t \geq 0. \tag{55}$$

Let $\Omega_0 = \{(\psi_1,\psi_2,\psi_3,\psi_4) \in X^+ : \psi_2 \not\equiv 0 \text{ or } \psi_4 \not\equiv 0\}$ and $\partial\Omega_0 = X^+\backslash\Omega_0 = \{(\psi_1,\psi_2,\psi_3,\psi_4) \in X^+ : \psi_2 \equiv 0 \text{ and } \psi_4 \equiv 0\}$. Clearly, Ω_0 and $\partial\Omega_0$ are relatively open and closed subsets of X^+. Furthermore, $X^+ = \Omega_0 \cup \partial\Omega_0$ and $\Omega_0 \cap \partial\Omega_0 = \emptyset$. Clearly, Ω_0 is convex and $\Phi_t(A) \subset A$ where $A = \Omega_0$ or $\partial\Omega_0$ for $t \geq 0$. In view of Lemma 4.3, we can conclude that Φ_t is a periodic semiflow on X^+, and for each $t > 0$, $\Phi_t : X^+ \to X^+$ is compact. Furthermore, by Lemma 4.3, the standard argument similar to the proof of [9, Theorem 23.3] yields that the map Φ_t is point dissipative in X^+.

In what follows, we will prove the uniform persistence for the Poincaré map defined by

$$\begin{array}{rccc} P: & X^+ & \longrightarrow & X^+ \\ & u_0 & \longmapsto & \Phi_\omega(u_0). \end{array} \tag{56}$$

With the above argument, one can easily verify that $P : X^+ \to X^+$ is continuous, compact and point dissipative. By Lemma 4.3 and [45, Theorem1.1.3], $P : X^+ \to X^+$ has a strong global attractor.

Next, we want to show that $\tilde{\omega}(u_0) = \{\mathcal{E}_0\}$ for any $u_0 \in \partial\Omega_0$, where $\tilde{\omega}(u_0)$ is the omega limit set of the forward orbit through u_0 for $P : X^+ \to X^+$ and $\mathcal{E}_0 := (\bar{N}, 0, 0, 0)$. If $u_0 := (S_0, I_0, R_0, B_0) \in \partial\Omega_0$, then $\Phi_t(u_0) := (S,I,R,B) \in \partial\Omega_0$ and hence $I \equiv B \equiv 0$ for $t \geq 0$. By the third equation of (1), $\lim_{t\to\infty} R(x,t) = 0$ uniformly for $0 \leq x \leq 1$. Thus, S is asymptotic to $\bar{S}$, where $\bar{S}$ is the solution of (50) and $\lim_{t\to\infty} \bar{S}(x,t) = \bar{N}$. It follows from the theory of asymptotic autonomous semiflow [28, Corollary 4.3] that $\lim_{t\to\infty} S(x,t) = \bar{N}$. This shows that $\bigcup_{u_0\in\partial\Omega_0} \tilde{\omega}(u_0) = \{\mathcal{E}_0\}$ and $\mathcal{E}_0$ is compact and isolated invariant set for the Poincaré map P in M, where M is the largest positively invariant set of $P : \partial\Omega_0 \to \partial\Omega_0$.

ACCEPTED MANUSCRIPT

Let μ_η be the unique principle eigenvalue of the periodic-parabolic problem

$$\begin{aligned}
&\frac{\partial \phi_I}{\partial t} = H_I(\phi_I, \phi_B, \eta) + D_2 \frac{\partial^2 \phi_I}{\partial x^2} + \mu_\eta \phi_I, && 0 < x < 1,\ t > 0,\\
&\frac{\partial \phi_B}{\partial t} = H_B(\phi_I, \phi_B, \eta) - v\frac{\partial \phi_B}{\partial x} + D_4 \frac{\partial^2 \phi_B}{\partial x^2} + \mu_\eta \phi_B, && 0 < x < 1,\ t > 0,\\
&\frac{\partial \phi_I}{\partial x} = 0,\ D_4 \frac{\partial \phi_B}{\partial x} - v\phi_B = 0, && x = 0, 1,\ t > 0,\\
&(\phi_I, \phi_B)(x, 0) = (\phi_I, \phi_B)(x, \omega), && 0 < x < 1,
\end{aligned} \tag{57}$$

with

$$\begin{aligned}
H_I(\phi_I, \phi_B, \eta) &= \beta_1(x,t)(\bar{N} - \eta)\phi_I + \frac{\beta_2(x,t)(\bar{N} - \eta)\phi_B}{\eta_0 + K} - (d + \gamma)\phi_I\\
H_B(\phi_I, \phi_B, \eta) &= \xi(x,t)(\bar{N} - \eta) + g(x,t)\phi_B\left(1 - \frac{\eta}{K_B}\right) - \delta\phi_B.
\end{aligned} \tag{58}$$

Particularly, μ_0 is defined in the preceding section. Applying Lemma 3.1, we know that $\mu_0 < 0$ under the assumption $R_0 > 1$. By the continuity of the principle eigenvalue with respect the weight functions, there exists $\eta_0 > 0$ sufficiently small such that $\mu_{\eta_0} < 0$. We now claim that $\mathcal{E}_0$ is a uniform weak repeller for Ω_0 in the sense that

$$\limsup_{n\to\infty} \|P^n(u_0) - \mathcal{E}_0\|_{X^+} \geq \eta_0, \quad \forall\, u_0 \in \partial\Omega_0. \tag{59}$$

By the continuous dependence of solution on the initial data, we see that

$$\lim_{u_0 \to \mathcal{E}_0} \Phi_t(u_0) = \lim_{u_0 \to \mathcal{E}_0} u(\cdot, t, u_0) = \mathcal{E}_0 \tag{60}$$

in X^+ uniformly for all $t \in [0, \omega]$. Thus, there exists $\delta_0 = \delta_0(\eta_0)$, such that for any $u_0 \in B(\mathcal{E}_0, \delta_0)$,

$$u(\cdot, t, u_0) \in B(\mathcal{E}_0, \eta_0), \quad t \in [0, \omega], \tag{61}$$

where $B(\mathcal{E}_0, r)$ denotes the open ball in X^+ centered at $\mathcal{E}_0$ with a radius r. We'll now verify the assertion (59) by a contradiction argument. Suppose that there exists $\hat{u}_0 = (\hat{S}_0, \hat{I}_0, \hat{R}_0, \hat{B}_0) \in B(\mathcal{E}_0, \delta_0) \cap \Omega_0$ such that $P^n(\hat{u}_0) = \Phi_{n\omega}(\hat{u}_0) \in B(\mathcal{E}_0, \eta_0) \cap \Omega_0$ for any $n \geq 1$. For all $t \geq 0$, we write $t = n\omega + \hat{t}$, where n is the largest integer less than or equal to t/ω and $\hat{t} \in [0, \omega)$. In view of $(\hat{S}, \hat{I}, \hat{R}, \hat{B})(\cdot, t) := \Phi_t(\hat{u}_0) = \left(\Phi_{\hat{t}} \circ \Phi_{n\omega}\right)(\hat{u}_0)$, we have

$$(\hat{S}, \hat{I}, \hat{R}, \hat{B})(\cdot, t) \in B(\mathcal{E}_0, \eta_0), \quad t \geq 0. \tag{62}$$

Let V_{η_0} be the strongly positive eigenfunction corresponding to the principle eigenvalue μ_{η_0}, and $\mathrm{int}(Z^+)$ denote the interior of Z^+ for $Z = X, Y$. Then $V_{\eta_0}(\cdot, 0) \in \mathrm{int}(Y^+) \times \mathrm{int}(Y^+)$. Since $\hat{u}_0 \in \Omega_0$, we have known $\hat{S}(\cdot, t), \hat{I}(\cdot, t), \hat{R}(\cdot, t)$, and $\hat{B}(\cdot, t) \in \mathrm{int}(\mathrm{Y}^+)$ for $t > 0$ by using the strong maximal principle. Without loss of generality, we may assume that $\hat{I}_0, \hat{B}_0 \in \mathrm{int}(\mathrm{Y}^+)$. Then, there exists a constant $c_0 > 0$ such

ACCEPTED MANUSCRIPT

that $(\hat{I}_0, \hat{B}_0)(x) \geq c_0 V_{\eta_0}(x,0)$ for $x \in [0,1]$. In view of (62), we see that $(\hat{I}, \hat{B})$ is a super-solution to the following problem

$$\begin{aligned}
&\frac{\partial \psi_I}{\partial t} = H_I(\psi_I, \psi_B, \eta_0) + D_2 \frac{\partial^2 \psi_I}{\partial x^2}, && 0 < x < 1,\ t > 0,\\
&\frac{\partial \psi_B}{\partial t} = H_B(\psi_I, \psi_B, \eta_0) - v\frac{\partial \psi_B}{\partial x} + D_4 \frac{\partial^2 \psi_B}{\partial x^2}, && 0 < x < 1,\ t > 0,\\
&\frac{\partial \psi_I}{\partial x} = 0,\ D_4 \frac{\partial \psi_B}{\partial x} - v\psi_B = 0, && x = 0, 1,\ t > 0,\\
&(\psi_I, \psi_B)(x,0) = c_0 V_{\eta_0}(x,0), && 0 < x < 1
\end{aligned} \tag{63}$$

where H_I and H_B are defined in equation (58).

Since $c_0 e^{-\mu_{\eta_0} t} V_{\eta_0}(x,t)$ is the unique solution to problem (63), the comparison principle particularly implies that

$$(\hat{I}, \hat{B})(x,t) \geq c_0 e^{-\mu_{\eta_0} t} V_{\eta_0}(x,t), \quad \text{uniformly for } x \in [0,1], \text{ as } t \to \infty, \tag{64}$$

which contradicts to (62) as $\mu_{\eta_0} < 0$. Thus this proves the claim (59).

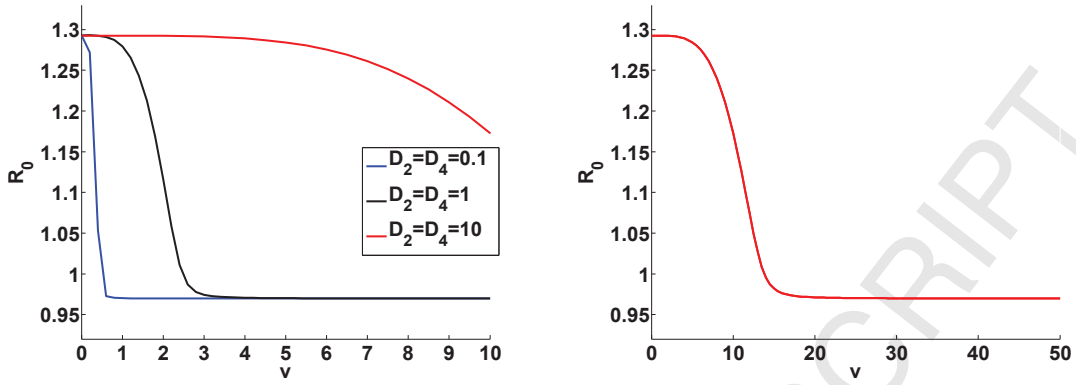
From the above claim, we see that $\{\mathcal{E}_0\}$ is an isolated invariant set for the Poincaré map $P : X^+ \to X^+$ and $W^S(\mathcal{E}_0) \cap \Omega_0 = \emptyset$, where $W^S(\mathcal{E}_0)$ refers to the stable set of $\mathcal{E}_0$ for $P : X^+ \to X^+$. Therefore, it follows from [45, Theorem 1.3.1 and Remark 1.3.1] that P is uniformly persistent with respect to $(\Omega_0, \partial\Omega_0)$. Consequently, [19, Theorem 4.5] implies that P has a fixed point u^* in Ω_0, and hence system (1) has an ω-periodic solution $\phi_t(u^*)$ in Ω_0. By [19, Theorem 4.5] , we further see that $P : \Omega_0 \to \Omega_0$ has a compact global attractor A_0. It is clear that $u^* \in A_0$. Write $B_0 = \bigcup_{0 \leq t < \omega} \Phi_t A_0$. Then $B_0 \in \Omega_0$ and [45, Theorem 3.1.1] implies that $\lim_{t\to\infty} d(\Phi_t(u_0), B_0) = 0$ for all $u_0 \in \Omega_0$, where d is the norm induced distance in $Y \times Y \times Y \times Y$. Since $A_0 \subset \Omega_0$ and $A_0 = P(A_0) = \Phi_\omega(A_0)$, we see that $A_0 \in \text{int}(X^+)$ and hence $B_0 \in \text{int}(X^+)$. As $\Phi_t(u^*) \in B_0$, $\Phi_t(u^*)$ is a positive ω-periodic solution of system (1). By the compactness and global attractiveness of B_0 for Φ_t in X^+, we conclude that there exists $\eta^* > 0$ such that $\liminf_{t\to\infty} \Phi_t(u_0) \geq (\eta^*, \eta^*, \eta^*, \eta^*)$ for all $u_0 \in \Omega_0$. This completes the proof. □

5. Numerical Results

In this section, we apply the numerical method described in the Appendix to compute the basic reproduction number R_0 of our model and demonstrate some of our analytical results. Our focus is the impact of the model parameter associated with for the seasonal factors (reflecting the temporal variation) and the diffusion and convection rates (representing the spatial movement) on the value of R_0. Specifically, we set $\beta_i(\cdot,t) = \beta_{i0} + \beta_{i1}\sin(2\pi t/T)$ (for $i = 1, 2$), $\xi(\cdot,t) = \xi_0 + \xi_1 \sin(2\pi t/T)$ and $g(\cdot,t) = g_0 + g_1 \sin(2\pi t/T)$ with $T = 365$ days, for $t \geq 0$ on $[0,1]$, where β_{i0}, β_{i1} $(i = 1, 2)$, ξ_0, ξ_1, g_0, and g_1 are all nonnegative constants.

Figure 1 illustrates the influence of the convection and diffusion rates on the disease risk. For simplicity, we set $D_2 = D_4$, and plot the basic reproduction number R_0 versus the bacterial convection rate v for three scenarios: (1) small diffusion: $D_2 = D_4 = 0.1$;

ACCEPTED MANUSCRIPT



(a) (b) $D_2 = D_4 = 10$

Figure 1: Influence of v and D_4 on R_0 when $D_2 = D_4$, which is illustrated by plotting R_0 as a function of v for different values of D_4. The parameter values are mainly taken from [21] and given by $d = (43.5\text{y})^{-1}, \gamma = (5\text{d})^{-1}, \sigma = (3\text{y})^{-1}, \delta = (30\text{d})^{-1}, K = 10^6$ cells·ml^{-1} and $K_B = 2 \times 10^6$. All diffusion efficients have a unit of km^2 d^{-1} and the unit of the bacterial advection v is km d^{-1}. The base values of indirect and direct transmission rates, shedding rate and intrinsic growth rate of pathogen are $\beta_{10} = 1.1 \times 10^{-4}$ (person^{-1}week^{-1}), $\beta_{20} = .075 \times 10^{-4}$ (week^{-1}), $\xi_0 = 0.71$ (cells ml^{-1}week^{-1}) and $g_0 = 0.3$ (week^{-1}). Here $\beta_{i1} = \beta_{i0}/5$ $(i = 1, 2)$, $\xi_1 = \xi_0/2$ and $g_1 = g_0/2$.

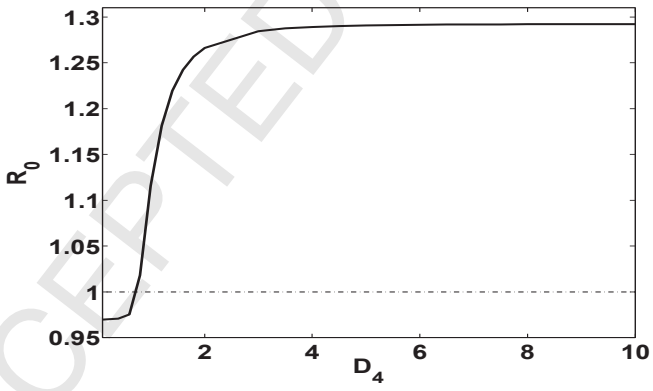


Figure 2: Impact of D_4 on R_0 with $D_2 = 1$ and $v = 1$. The dash-dot line shows where $R_0 = 1$.

(2) moderate diffusion: $D_2 = D_4 = 1$; and (3) large diffusion: $D_2 = D_4 = 10$. We observe that as D_2 and D_4 become larger, the value of R_0 grows, indicating that a stronger diffusion process tends to increase the infection risk, as the pathogens and infected hosts are dispersed on a faster pace which may lead to a higher degree of disease contacts through both the direct and indirect routes. On the other hand, the bacterial convection seems to have an opposite effect on the infection risk: as v increases, R_0 first decreases, and then approaches a constant level slightly lower than

ACCEPTED MANUSCRIPT

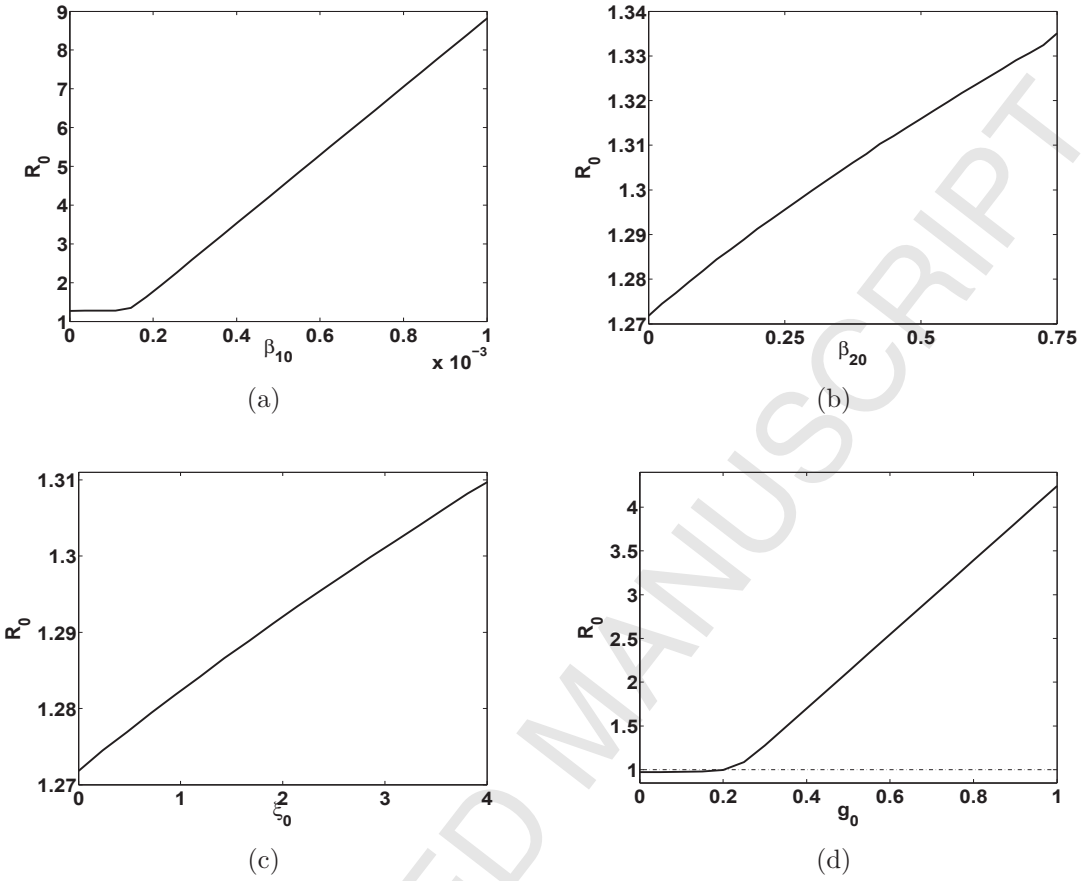


Figure 3: Impact of the base value of β_{10}, β_{20} and ξ_0 and g_0 on R_0 when $D_2 = D_4 = v = 1$. In (d), the dash-dot line displays where $R_0 = 1$.

unity. A possible explanation is that as the convection rate becomes larger, the bacteria are transported faster from the upstream to the downstream through the river flow, thus reducing the average time of contacts between the pathogen and the human hosts and leading to a lower disease risk. We also notice that for each of the three choices of the diffusion rates, there seems to exist a critical convection speed, say $v*$, such that when $v < v*$, R_0 keeps decreasing; and when $v > v*$, R_0 is stabilized at a fixed point. The value of $v*$ depends on the strength of the diffusion: when D_2 and D_4 increase, $v*$ also increases, to a level of balance where the convection is strong enough to offset the effects of the diffusion. Additionally, Figure 2 illustrates a scenario where $D_2 \neq D_4$. We again observe that the value of R_0 increases as D_4 gets larger, while D_2 and v are fixed.

Figures 3 and 4 display the variation of R_0 with respect to several parameters in the time-dependent and periodically oscillating contact and growth rates. It is clear to see a general growth pattern of R_0 as these parameters (including both the base values and oscillation amplitudes) increase, showing the positive effects of the temporal fluctuation

ACCEPTED MANUSCRIPT

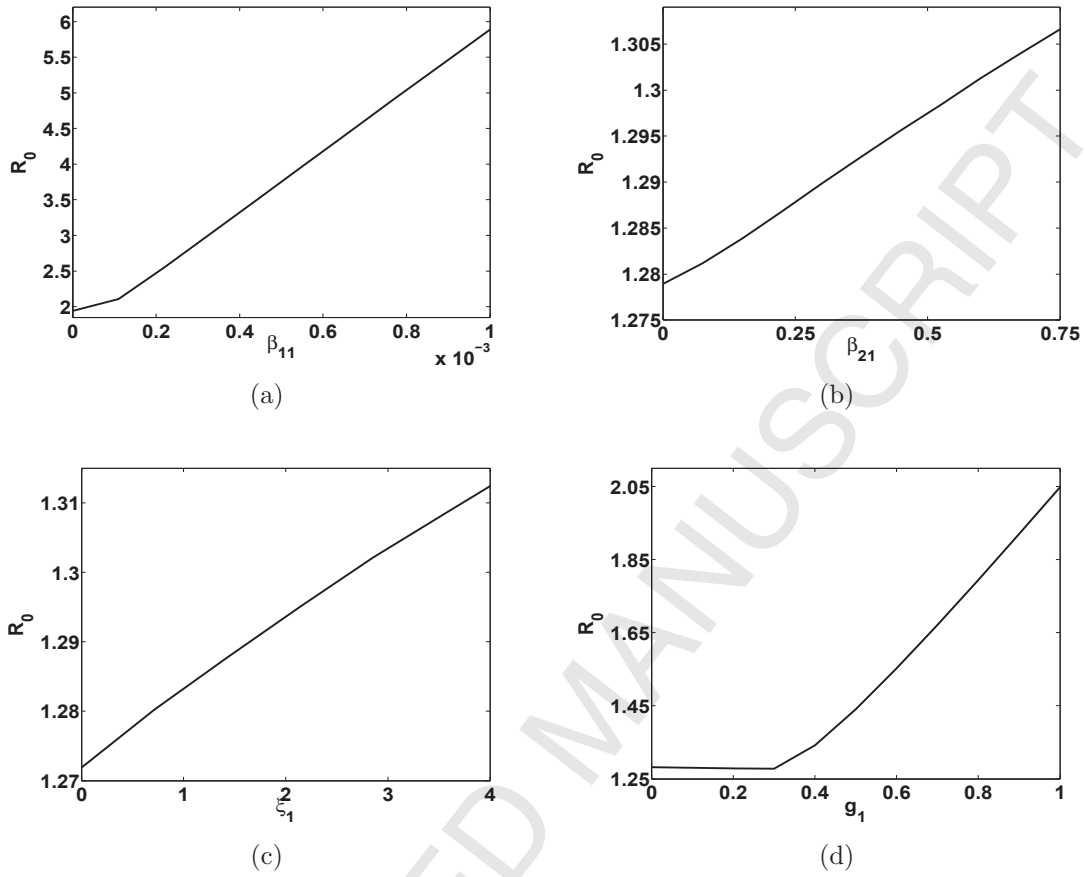


Figure 4: Impact of the base value of β_{11}, β_{21} and ξ_1 and g_1 on R_0. Here $D_2 = D_4 = v = 1$. $\beta_i = \max\{\beta_{i0} + \beta_{i1}\sin(2\pi t/T), 10^{-4}\}$ $(i = 1, 2)$, $\xi = \max\{\xi_0 + \xi_1 \sin(2\pi t/T), 10^{-4}\}$ and $g = \max\{g_0 + g_1 \sin(2\pi t/T), 10^{-4}\}$. The base values of indirect and direct transmission rates, shedding rate and intrinsic growth rate of pathogen are $\beta_{10} = 1.1 \times 10^{-4}$ (person^{-1}week^{-1}), $\beta_{20} = 0.075$ (week^{-1}), $\xi_{10} = 0.71$ (cells ml^{-1}week^{-1}) and $g_0 = 0.3$ (week^{-1}).

on the elevation of the disease risk. An indication is that if such seasonal variation is not taken into account in the calculation of the basic reproduction number, we would under-estimate the risk of the infection.

6. Discussion

We have presented a new modeling framework for the transmission dynamics of cholera, based on a SIR-B (susceptible-infected-recovered-bacteria) compartment structure. Our model utilizes the reaction-convection-diffusion processes to represent the spatial movement of the hosts and pathogens, and the periodic contact and growth rates to describe the seasonality of the disease transmission, thus incorporating both the spatial and seasonal dynamics in a single framework. Using the next generation operator, we have introduced the basic reproduction number, R_0 , for our periodic

ACCEPTED MANUSCRIPT

PDE cholera model and conducted a careful analysis, based on the theory of monotone dynamical systems [45] and the persistence theory [44, 19]. Consequently, we have established the condition $R_0 = 1$ as a threshold for characterizing the cholera dynamics in such a spatiotemporally heterogeneous environment. In particular, we have shown that when $R_0 < 1$, the disease-free solution is globally asymptotically stable; when $R_0 > 1$, the system is uniformly persistent and there exists a positive periodic solution.

Our periodic PDE framework can potentially incorporate a wide range of epidemiologically relevant factors, including biological (e.g., intrinsic bacterial growth and death), environmental (e.g., host shedding and pathogen dispersal), geographical (e.g., locational difference in ecology and demographics), climatic (e.g., seasonal fluctuation), and physical (e.g., human and bacterial diffusion/convection). Our model also allows us to consider multiple transmission pathways for cholera that includes both human-to-human (direct) and environment-to-human (indirect) routes. These make it possible to study the complex interaction among many simultaneous and coupled processes that contribute to the whole picture of cholera transmission dynamics, in a single framework and through a holistic manner.

We have paid special attention to the basic reproduction number, R_0 , as the means to characterize the disease threshold. Although an analytical solution for R_0, which is defined as the spectral radius of the next generation operator, is impossible in general, we have developed a novel algorithm to compute R_0 numerically by solving the associated principal eigenvalue problem. We have obtained simulation results for R_0 with the variation of a number of key model parameters. Our numerical results show that while the host movement and pathogen dispersal (represented by a diffusion process in our model) tend to increase the infection risk, the transport of pathogens through the river flow (represented by a convection process) seems to have a counter effect. From the practical point of view, the convection process through the river flow may be difficult to control, and our results suggest that the disease control measures could be focused more on the diffusion process to reduce the risk of cholera infection. For example, reducing the activity levels of infected individuals and limiting their travel to other places could weaken the host "diffusion", and using water sanitation as a disease prevention/intervention method could reduce the pathogen dispersal. Meanwhile, our results also demonstrate that R_0 increases when the temporal oscillation of model parameters becomes stronger. These findings imply that an accurate representation of R_0 can only be obtained through the incorporation of both spatial and temporal factors, and neglecting any of these might lead to incorrect estimate (particularly, under-estimate) of the infection risk. The results also indicate that the prevention and intervention strategies need to take into account the spatial and temporal heterogeneities in order to effectively control cholera while optimize the use of available resources.

Our current study on the spatial modeling of cholera is based on a reaction-convection-diffusion PDE system. A different approach is to utilize a patch structure, where the entire system is divided into a number of patches that represent different spatial characteristics. Within each patch, spatial homogeneity is assumed and an ODE

ACCEPTED MANUSCRIPT

system can be constructed to represent the disease dynamics, taking into account the communication and movement of hosts and/or pathogens across different patches. Seasonal variation can be similarly incorporated by considering periodic model parameters for each patch, resulting in a multi-patch periodic ODE system. It will be very interesting to compare the threshold dynamics of cholera from these two modeling approaches: one based on periodic PDEs, and the other based on multi-patch periodic ODEs. We plan to purse this research task in our future work.

Appendix. A numerical algorithm for R_0

To numerically solve the principle eigenvalue of (32), we discretize the space uniformly and write $u_i(t) = \phi(x_i, t)$ with $x_i = i/(n-1)$ with $0 \le i \le n-1$. Employ the finite difference method to the spatial differential operator. The original eigenvalue problem (32) can be written in the following

$$\frac{du}{dt} = Au + \lambda B(t)u, \tag{65}$$

where $u = (u_0, u_1, \cdots, u_{n-1})$, A is an $n \times n$ constant matrix and B is an $n \times n$ matrix function on $[0,1] \times [0, \omega)$.

Now we consider a more general problem

$$\frac{du}{dt} = Au + \lambda B(t)u + \mu(\lambda)u. \tag{66}$$

To solve (65), it is sufficient to find λ_0 such that $\mu(\lambda_0) = 0$.

Denote $M(\lambda, \mu, t) = A + \lambda B(t) + \mu(\lambda)$. Let $X(\lambda, \mu, t)$ be the fundamental solution of $\dfrac{dY}{dt} = M(\lambda, \mu, t)Y$, which satisfies

$$\frac{dX}{dt} = M(\lambda, \mu, t)X, \quad X(\lambda, \mu, 0) = I_n, \tag{67}$$

for which I_n is the identity matrix of size n. Thus,

$$u(t) = X(\lambda, \mu, t)u(0). \tag{68}$$

Since $u(t)$ is ω-period, we have

$$u(0) = X(\lambda, \mu, \omega)u(0). \tag{69}$$

It follows from $u(0) \gg 0$ that

$$\rho(X(\lambda, \mu, \omega)) = 1. \tag{70}$$

Suppose λ^* is the eigenvalue of (65). Then $\mu(\lambda^*) = 0$ and

$$\rho(X(\lambda^*, \mu(\lambda^*), \omega)) = \rho(X(\lambda^*, 0, \omega)) = 1. \tag{71}$$

Therefore, to solve (32) numerically, it suffices to find λ^* such that

$$\rho(X(\lambda^*, 0, \omega)) = 1. \tag{72}$$

It follows from Lemma 3.2 that $R_0 = 1/\lambda^*$.

ACCEPTED MANUSCRIPT

Acknowledgements

This research was initiated at an AIM SQuaRE, and the authors acknowledge the AIM for providing financial support and an excellent working environment. The authors also thank anonymous reviewers and the editor for their suggestions that improved this paper. X.W. is partially supported by a Grant from the Simons foundation (No. 317407); X.-Q.Z. acknowledges the support of the NSERC of Canada; J.W. is supported in part by National Science Foundation (Nos. 1412826 and 1557739).

References

[1] J. R. Andrews, S. Basu, Transmission dynamics and control of cholera in Haiti: an epidemic model, *Lancet*, 377 (9773) (2011) 1248-1255.

[2] N. Bacaër, S. Guernaoui, The epidemic threshold of vector-borne diseases with seasonality. J. Math. Biol. 53 (2006) 421-436.

[3] Alex Beltramo, Peter Hess, On the principal eigenvalue of a periodic-parabolic operator, Communications in Partial Differential Equations, 9:9 (1984) 919-941.

[4] E. Bertuzzo, R. Casagrandi, M. Gatto, I. Rodriguez-Iturbe and A. Rinaldo, On spatially explicit models of cholera epidemics, Journal of the Royal Society Interface, 7 (2010) 321-333.

[5] V. Capasso, L. Maddalena, Convergence to equilibrium states for a reactiondiffusion system modeling the spatial spread of a class of bacterial and viral diseases. J Math Biol 13 (1981) 173-184.

[6] V. Capasso, S. L. Paveri-Fontana, A mathematical model for the 1973 cholera epidemic in the European Mediterranean region, Rev. Epidemiol. Sante, 27(2) (1979) 121-132.

[7] F. Capone V. De Cataldis R. De Luca , Influence of diffusion on the stability of equilibria in a reaction-diffusion system modeling cholera dynamic, J. Math. Biol. 71 (2015) 1107-1131.

[8] C.T. Codeço, Endemic and epidemic dynamics of cholera: the role of the aquatic reservoir, BMC Infect. Dis., 1:1 (2001).

[9] D. Daners and K. Medina, Abstract Evolution Equations, Periodic Problems and Applications(Pitman Research Notes in Mathematics Series vol 279) (Harlow: Longman Scientific & Technical), 1992.

[10] O. Diekmann, J.A.P. Heesterbeek, A.J. Metz, On the definition and the computation of the basic reproduction ratio R_0 in models for infectious diseases in heterogeneous population, J. of Math. Bio., 28 (1990) 365-382.

ACCEPTED MANUSCRIPT

[11] D. Le (1997) Dissipativity and global attractors for a class of quasilinear parabolic systems Commun. Partial Diff. Eqns 22, 413-33.

[12] M.C. Eisenberg, Z. Shuai, J.H. Tien, and P. van den Driessche, A cholera model in a patchy environment with water and human movement, Math. Biosci., 246 (2013) 105-112.

[13] M. Gatto, L. Mari, L. and A. Rinaldo, Leading eigenvalues and the spread of cholera. SIAM News, 46(7) (2013).

[14] D. M. Hartley, J. G. Morris, D. L. Smith, Hyperinfectivity: a critical element in the ability of *V. cholerae* to cause epidemics? PLoS Med., 3 (2006) 0063-0069.

[15] A.A. King, E.L. Ionides, M. Pascual, M. J. Bouma MJ, Inapparent infections and cholera dynamics. Nature 454 (2008): 877-880.

[16] Y. Lou and X.-Q. Zhao, A theoretical approach to understanding population dynamics with seasonal developmental durations, J. Nonlinear Sci., 27 (2017) 573-603.

[17] S. Islam, S. Rheman, A.Y. Sharker, et al., Climate change and its impact on transmission dynamics of cholera, Climate Change Cell, DoE, MoEF; Component 4B, CDMP, MoFDM, Dhaka, 2009.

[18] P. Hess, Periodic-parabolic boundary value problems and positivity, Pitman Research, Notes in Mathematics 247. Longman Sci. Tech., Harlow, 1991.

[19] P. Magal and X. -Q. Zhao, Global attractors and steady states for uniformly persistent dynamical systems, SIAM. J. Math. Anal., 37 (2005) 251-275.

[20] R. Peng, X.-Q. Zhao, A reaction-diffusion SIS epidemic model in a time-periodic environment, Nonlinearity 25 (2012) 1451-1471.

[21] Z. Mukandavire, S. Liao, J. Wang, H. Gaff, D. L. Smith, J. G. Morris, Estimating the reproductive numbers for the 2008-2009 cholera outbreaks in Zimbabwe, Proc. Nat. Acad. Sci. USA, 108 (2011) 8767-8772.

[22] E. J. Nelson, J. B. Harris, J. G. Morris, S. B. Calderwood, A. Camilli, Cholera transmission: the host, pathogen and bacteriophage dynamics, Nat. Rev. Microbiol., 7 (2009) 693-702.

[23] D. Posny, J. Wang, Modelling cholera in periodic environments, J. Biol. Dyn., 8(1) (2014) 1-19.

[24] M. H. Protter and H. F. Weinberger, Maximum Principles in Differential Equations, Corrected reprint of the 1967 original, Springer-Verlag, New York, 1984.

ACCEPTED MANUSCRIPT

[25] A. Rinaldo, E. Bertuzzo, L. Mari, L. Righetto, M. Blokesch, M. Gatto, R. Casagrandi, M. Murray, S.M. Vesenbeckh, and I. Rodriguez-Iturbe, Reassessment of the 2010-2011 Haiti cholera outbreak and rainfall-driven multiseason projections, Proc. Nat. Acad. Sci. USA, 109 (2012) 6602-6607.

[26] Z. Shuai, J.H. Tien and P. van den Driessche, Cholera models with hyperinfectivity and temporary immunity, Bull. Math. Biol., 74 (2012) 2423-2445.

[27] Z. Shuai and P. van den Driessche, Modeling and control of cholera on networks with a common water source, Journal of Biological Dynamics, Vol. 9, Suppl. 1 (2015) 90-103.

[28] H. R. Thieme, Convergence results and Poincare-Bendixson trichotomy for asymptotically autonomous differential equations, J. Math. Biology, 30 (1992) 755-763.

[29] H. R. Thieme, Spectral bound and reproduction number for infinite-dimensional population structure and time heterogeneity, SIAM J. Appl. Math., **70** (2009) 188-211.

[30] J. P. Tian, J. Wang, Global stability for cholera epidemic models Math. Biosci., 232(1) (2011) 31-41.

[31] J. H. Tien, D. J. D. Earn, Multiple transmission pathways and disease dynamics in a waterborne pathogen model, Bull. Math. Biol., 72(6) (2010) 1506-1533.

[32] A.R. Tuite, J.H. Tien, M.C. Eisenberg, D.J.D. Earn, J. Ma, D.N. Fisman, Cholera epidemic in Haiti, 2010 – Using a transmission model to explain spatial spread of disease and identify optimal control interventions, Annals of Internal Medicine, 154(9) (2011) 593-601.

[33] P. van den Driessche, J. Watmough, Reproduction numbers and sub-threshold endemic equilibria for compartmental models of disease transmission. Math. Biosci. 180 (2002) 29-48.

[34] X. Wang, D. Gao and J. Wang, Influence of human behavior on cholera dynamics, Mathematical Biosciences, 267 (2015) 41-52.

[35] J. Wang, S. Liao, A generalized cholera model and epidemic-endemic analysis, J. Biol. Dyn., 6(2) (2012) 568-589.

[36] X. Wang and J. Wang, Analysis of cholera epidemics with bacterial growth and spatial movement, J. Biol. Dyn., 9:S1 (2015) 233-261.

[37] W. Wang, X.-Q. Zhao, Threshold dynamics for compartmental epidemic models in periodic environments. J. Dyn. Diff. Equ. 20 (2008) 699717.

ACCEPTED MANUSCRIPT

[38] S.O. Wandiga, Climate change and induced vulnerability to malaria and cholera in the Lake Victoria region, AIACC Final Report, Project No. AF 91, Published by The International START Secretariat, Washington, DC, USA, 2006.

[39] W. Wang and X.-Q. Zhao, Basic reproduction numbers for reaction-diffusion epidemic models, SIAM Journal on Applied Dynamical Systems, 11 (2012) 1652-1673.

[40] K. Yamazaki, X. Wang, Global well-posedness and asymptotic behavior of solutions to a reaction-convection-diffusion cholera epidemic model, Discrete Contin. Dyn. Syst. Ser. B 21 (2016) 1297-1316.

[41] K. Yamazaki and X. Wang, Global stability and uniform persistence of the reaction-convection-diffusion cholera epidemic model, Math. Biosci. Eng., 14:2 (2017) 559-579.

[42] X. Yu and X.-Q. Zhao, A nonlocal spatial model for Lyme disease, Journal of Differential Equations, 261 (2016) 340-372.

[43] World Health Organization (WHO) web page: http://www.who.org.

[44] X.-Q. Zhao, Uniform persistence and periodic coexistence states in infinite-dimensional periodic semiflows with applications, Can. Appl. Math. Q. 3 (1995) 473-495.

[45] X.-Q. Zhao, Dynamical Systems in Population Biology, New York, Springer, 2003.

ACCEPTED MANUSCRIPT